Lung Cancer 150 (2020) 132–138

Contents lists available at ScienceDirect

Lung Cancer

journal homepage: www.elsevier.com/locate/lungcan

Deciphering the clonal relationship between glandular and squamous components in adenosquamous carcinoma of the lung using whole exome sequencing

Arthur Krause [a,1], Luca Roma [a,1], Thomas Lorber [a], James Habicht [b], Didier Lardinois [c], Maria Rosaria De Filippo [a,f], Spasenija Savic Prince [a], Salvatore Piscuoglio [a,d], CharlotteKY Ng [e], Lukas Bubendorf [a,*]

[a] Institute of Molecular Genetics and Pathology, University Hospital Basel, University of Basel, Switzerland
[b] Thoracic Surgery, St. Clara Hospital, Basel, Switzerland
[c] Thoracic Surgery, University Hospital Basel, Basel, Switzerland
[d] Visceral Surgery Research Laboratory, Clarunis, Department of Biomedicine, University of Basel, Basel, Switzerland
[e] Department for BioMedical Research (DBMR), University of Bern, Bern, Switzerland
[f] Department for BioMedical Research, Urology Research Laboratory, University of Bern, Bern, Switzerland

ARTICLE INFO

Keywords:
Adenosquamous carcinoma
Lung cancer
Genomic evolution
Heterogeneity
STK11
SOX2

ABSTRACT

Adenosquamous carcinoma of the lung (ASC) is a rare subtype of non-small cell lung cancer, consisting of lung adenocarcinoma (LUAD) and lung squamous cell carcinoma (LUSC) components. ASC shows morphological characteristics of classic LUAD and LUSC but behaves more aggressively. Although ASC can serve as a model of lung cancer heterogeneity and transdifferentiation, its genomic background remains poorly understood. In this study, we sought to explore the genomic landscape of macrodissected LUAD and LUSC components of three ASC using whole exome sequencing (WES). Identified truncal mutations included the pan-cancer tumor-suppressor gene *TP53* but also *EGFR*, *BRAF,* and *MET*, which are characteristic for LUAD but uncommon in LUSC. No truncal mutation of classical LUSC driver mutations were found. Both components showed unique driver mutations that did not overlap between the three ASC. Mutational signatures of truncal mutations differed from those of the branch mutations in their descendants LUAD and LUSC. Most common signatures were related to aging (1, 5) and smoking (4). Truncal chromosomal copy number aberrations shared by all three ASC included losses of 3p, 15q and 19p, and an amplified region in 5p. Furthermore, we detected loss of *STK11* and *SOX2* amplification in ASC, which has previously been shown to drive transdifferentiation from LUAD to LUSC in preclinical mouse models. Conclusively, this is the first study using WES to elucidate the clonal evolution of ASC. It provides strong evidence that the LUAD and LUSC components of ASC share a common origin and that the LUAD component appears to transform to LUSC.

1. Introduction

Adenosquamous carcinoma (ASC) is a rare histological subtype of lung cancer accounting for 0.4 %–4 % of all lung cancers [1]. It consists of two morphologically distinct components including LUAD and LUSC [1]. From a clinical point of view, the biphasic ASC represents a challenge. It is more aggressive than its classical single components and has been shown to be associated with worse outcome [2]. There is no specific standard treatment for ASC, and current standard of care options rely on general non-small cell lung cancer (NSCLC) guidelines. Surgical resection is the only effective mean to treat patients with ASC, mostly in conjunction with platinum-based adjuvant chemotherapy [3]. Targeted treatments can be used as first-line therapy for advanced *EGFR*-mutant or *ALK*-rearranged ASC, but there are limited data on the efficacy of EGFR- or ALK-tyrosine kinase inhibitor (TKI) in ASC due to its rarity (reviewed in [4]). From a diagnostic perspective, it is challenging to grasp the biphasic nature of the tumor. Due to limited sampling by small biopsies, there is a high chance to miss one component so that the

* Corresponding author at: Institute of Medical Genetics and Pathology, University Hospital Basel, Schönbeinstrasse 40, 4031, Basel, Switzerland.
E-mail addresses: Lukas.Bubendorf@usb.ch, Luca.Roma@usb.ch (L. Bubendorf).
[1] Co-first author, contributed equally to the work

https://doi.org/10.1016/j.lungcan.2020.10.013
Received 29 July 2020; Received in revised form 17 October 2020; Accepted 17 October 2020
Available online 29 October 2020

subsequent treatment will be based on only one of the components.

Previous studies focusing on oncogenic driver mutations revealed that ASC have similar mutation profiles and therapeutic targets as LUAD including *EGFR* mutations [5,6]. Yet, to the best of our knowledge, the genomic profiles of the LUAD and LUSC components within ASC and the inferred evolutionary trajectories have not been explored previously, beyond the use of single gene and gene panel testing [5,6]. Being defined by its distinct morphological heterogeneity, ASC represents an ideal model to study morphological transdifferentiation and clonal evolution in NSCLC. Common LUAD is considered to originate from stem cells at the bronchoalveolar junction, whereas LUSC derive from the more proximally located basal cell compartment of the bronchial epithelium [7]. Based on targeted sequencing, several mutations were detected in both components LUAD and LUSC of ASC suggesting the two entities share the same ancestor cell [5,6]. It has been hypothesized that they are likely to arise at the bronchoalveolar junction as LUAD and that the LUSC phenotype develops subsequently [5,6]. The molecular mechanisms of this adenosquamous transdifferentiation (AST) remain unknown.

This study aims at better understanding the genomic landscape and the evolutionary trajectories of ASC. To this end, we dissected the LUAD and LUSC components separately from three ASC patients for comprehensive genomic profiling of both components using whole exome sequencing (WES).

2. Materials and methods

2.1. Patient cohort & immunohistochemistry

Three cases of ASC were retrieved from the pathology archive of the Institute of Pathology and Medical Genetics, University Hospital Basel, Switzerland. Representative formalin-fixed paraffin-embedded sections were cut (4 µm thick) and stained with hematoxylin and eosin. TTF-1, Napsin A, CK7 and p40 were used to distinguish LUAD and LUSC components. TTF-1 (Ventana catalog number 790–7456), Napsin A (Ventana catalog number 760–4867), CK7 (Ventana catalog number 790-4462) and p40 (Ventana catalog number 790–4950) staining was performed on the Benchmark Ultra (Ventana, Roche) as described previously [8]. The sections were reviewed by a pulmonary pathologist (LB), who marked distinct morphological regions for macrodissection. FISH analysis was performed according to the manufactures protocol (Zyto*Light*® SPEC SOX2/CEN3 dual color probe, catalog number Z-2127−200, Zytovision, Bremerhaven, Germany). This study has been carried out under the ethical approval EKNZ 31/12.

2.2. Macrodissection and DNA extraction

Up to ten consecutive 10 µm thick unstained tissue sections were cut on glass slides. The distinct morphological components and matched normal lung tissue were identified and marked by a pathologist (LB), scratched from the glass slide using a 25 g disposable syringe under a stereoscope as previously described [9]. Scratched cells were subjected to 200 µl of ATL buffer and 40 µl Proteinase K and incubated overnight at 56 °C with 500 rpm using the reagents from DNeasy Blood and Tissue Kit (Qiagen, Germantown, MD, USA) according to the manufacturer's instructions. DNA was quantified using the Qubit Fluorometer assay (Life Technologies, Carlsbad, CA, USA) as previously described [9].

2.3. Whole exome sequencing and variant annotation

Extracted DNA from normal and macrodissected ASC components were subjected to WES. SureSelect Human All Exon V6 Kit (Agilent) was used for the whole exome capturing according to manufacturer's guidelines. Sequencing was performed on Illumina NovaSeq 6000 using paired-end 100-bp reads and yielded a median depth of coverage of 48x to 120x in tumor components and 49x to 122x in the corresponding germlines (Supplementary Table 1). Sequencing was performed by CeGaT (Tübingen, Germany).

Reads were aligned to the reference human genome GRCh37. Somatic single nucleotide variants (SNVs) and small insertions and deletions (indels) were detected using MuTect (v.1.1.7) and Strelka (v.2.9.10), respectively [10,11]. To reduce false positive results from artifacts caused by formalin fixation, specific SNVs C:G > T:A with variant allelic fraction (VAF) less than 10 % were discarded. Otherwise, SNVs or indels with a VAF < 1% or that were covered by fewer than 3 reads were discarded, if the SNVs were found in both components of one sample, a cut-off of two read was applied. We further excluded variants identified in at least two of a panel of 123 non-tumor samples, including the non-tumor samples included in the current study. Variant annotation was performed by SnpEff software v.4.1 [12].

The heatmap of non-synonymous mutations was generated using the R package maftools v.2.0.16 by selecting the genes in the Bailey et al. dataset that represents the significantly mutated genes in classic LUAD and LUSC obtained from TCGA [13].

2.4. Copy number aberration analysis and clonality analysis

Allele-specific CNAs were identified using FACETS v.0.5.14 [14]. Deletions/losses were defined with the log-ratio < -0.3 and amplifications/gains > 0.3. Cancer cell fraction (CCF) of each mutation was identified using ABSOLUTE v.1.0.6 [15]. A mutation was classified as clonal if its probability of being clonal was > 50 % or if the lower bound of the 95 % confidence interval of its CCF was > 90 %. Mutations were considered as subclonal, if they did not meet the mentioned criteria [16,17]. A mutation that was found in both components of one biopsy was considered as 'trunk'. Mutations that were detected in only one component of the tumor were granted as 'branch' or 'private'.

2.5. Phylogenetic analysis and mutational signatures

A maximum parsimony tree was built for each case using binary presence/absence matrices based on the repertoire of non-synonymous and synonymous somatic mutations, gene amplifications and homozygous deletions in the biopsies of the tumors, as described by Murugaesu et al. [18,19].

Decomposition of mutational signatures was conducted using the R package deconstructSigs by selecting mutational signatures based on the set of 30 mutational signatures ('signature.cosmic') that were observed in LUAD and LUSC [20,21].

3. Results

3.1. Adenosquamous carcinoma have different growth patterns

The main clinico-pathologic characteristics of the three patients with ASC are summarized in Table 1. The three tumors were at stages pT2-pT4. In all three patients, the LUAD area was larger than the LUSC area. All LUSC areas were homogeneously p40-positive, while all LUAD areas were p40-negative by immunohistochemistry (Fig. 1). Two LUAD were TTF-1 positive (P118 & P119), while the other one was negative for both TTF1 and Napsin A. There was a predominant acinar growth pattern of the LUAD component in all three ASCs (Fig. 1 and Supplementary Fig. 2). Additional LUAD patterns were lepidic (P118 & P119) and solid (P119 & P120). Keratinization in the LUSC component was observed in P118 and P119.

3.2. LUAD and LUSC within adenosquamous carcinoma are of monoclonal origin

Overall, we found 759 non-synonymous mutations in 441 genes across the six tumor components of the three ASC. The proportion of shared mutations of LUSC and LUAD components of P118, P119 and

Table 1
Clinico-pathological features of the adenosquamous carcinomas at the time of resection.

Patient	P118	P119	P120
Age (at resection)	62	80	66
Sex	male	female	female
Smoking status	former	unknown	former
TNM classification	pT4 pNo cM0	pT2a pN0 cM0	pT3 pN1 cM0
Maximum Tumor diameter	8 cm	4.9 cm	8 cm
Lymphatic or venous invasion	no	no	yes (lymphatic & venous)
Pleural invasion	yes	yes	yes
Spread through air spaces (STAS)	no	no	no
Predominant LUAD pattern (%)	acinar (90 %)	acinar (80 %)	acinar (80 %)
Fraction of LUAD component	70 % (TTF1+)	60 % (TTF1+)	60 % (TTF1- & Napsin A -)
Fraction of LUSC component	30 % (p40+)	40+ (p40pos)	40+ (p40+)

P120 were 54 %, 28 % and 78 %, respectively (Fig. 2a, Supplementary table 2). The six separately analyzed tumor areas harbored a median of 72 (range 53–254) non-synonymous somatic mutations. Including synonymous mutations, the median of mutational burden was 3.5 mutations (mut)/Mb (range 2.3–11.6). It was highest in P120 (LUAD 11.6 mut/Mb and LUSC 11.3 mut/Mb) and lower in P118 (LUAD 3.5 mut/Mb, LUSC 2.3 mut/Mb) and P119 (LUAD 3.3 mut/Mb, LUSC 3.4 mut/Mb).

Across the samples, most of the mutations in driver genes were clonal (Fig. 2b). The analysis of P118 displayed four shared cancer gene mutations, of which only *EGFR* exon 19 deletion was clonal in both. *TP53* p. Gln192* was mutated in both components and a further *TP53* p. Gly108Asp mutation was detected only in the LUAD component. P119 shared three clonal mutations *MET, BRAF* and P119 *ACVR1B* mutations. We detected shared cancer gene mutations between the components of P120. Moreover, one clonal *STRN* mutation was detected in P120 LUAD. Further, four clonal and one subclonal private mutations were found in the LUSC component.

Gene copy number data from all patients and tumor components revealed high concordance between the two components (Fig. 2c).

3.3. Evolutionary history of genetic alterations

Most mutations in known cancer driver genes were truncal (Fig. 3). Most mutated cancer genes were known as typical for LUAD such as *EGFR, MET* and *BRAF*. P118 harbored a deletion in *EGFR* exon 19, a well-known driver gene in LUAD [6,22]. We found only KMT2D in P120, but not any other mutations in LUSC typical driver genes (Fig. 4). Interestingly, there were fewer mutations in the branches than truncal

Fig. 1. Adenosquamous carcinoma of the lung. Representative micrographs of a hematoxylin-eosin stained ASC (case P118) (a), the LUAD component immunostained with an antibody recognizing the lineage marker TTF-1 (**b**) and the LUSC immunostained with an antibody recognizing the specific marker p40 (**c**).

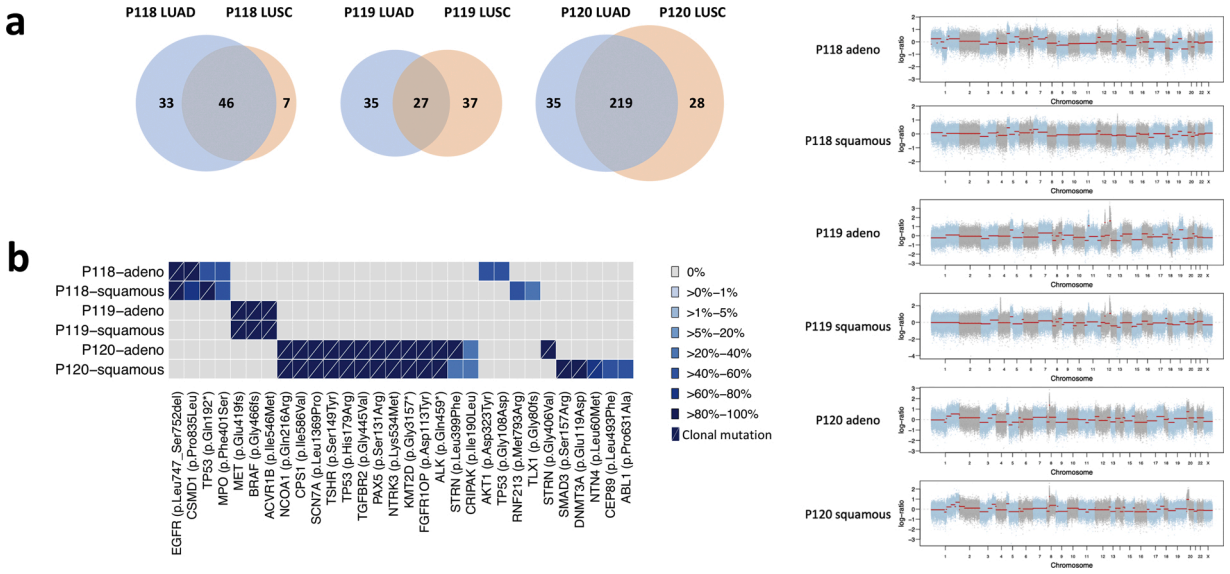

Fig. 2. LUAD and LUSC within adenosquamous carcinoma are of monoclonal origin. (**a**) Venn diagrams display the number of non-synonymous mutations per patient that are common between the LUAD (blue) and LUSC (red) components. The size of the circles is proportional to the number of mutations. (**b**) Heatmap illustrates the cancer cell fraction of selected mutations. Clonal mutations are illustrated with a diagonal line. (**c**) Copy number aberrations of every sample are displayed. (For interpretation of the references to colour in the Figure, the reader is referred to the web version of this article).

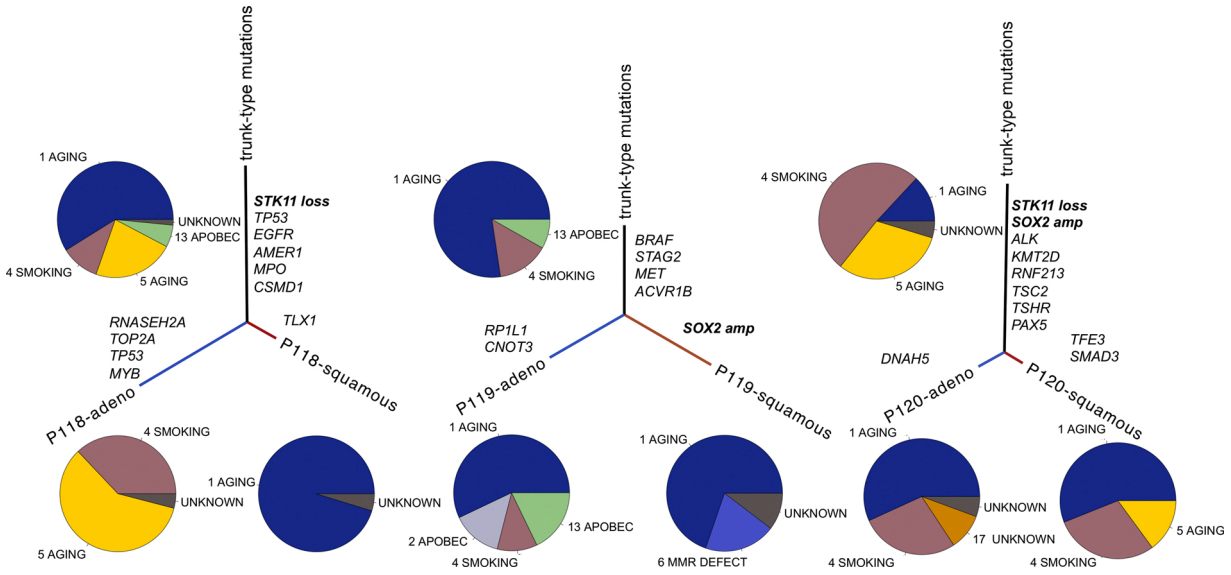

Fig. 3. Mutational signatures and genomic alterations of truncal and branch mutations in LUAD and LUSC. Evolution of the somatic genetic alterations illustrates the changes in mutational processes. Pie charts delineate the proportion of mutational signatures. Black, blue, and red lines represent the trunk, the LUAD branch, and the LUSC branch, respectively. Mutations or indels in cancer genes are noted next to branches. *STK11* loss and *SOX2* amplification are noted in bold. (For interpretation of the references to colour in the Figure, the reader is referred to the web version of this article).

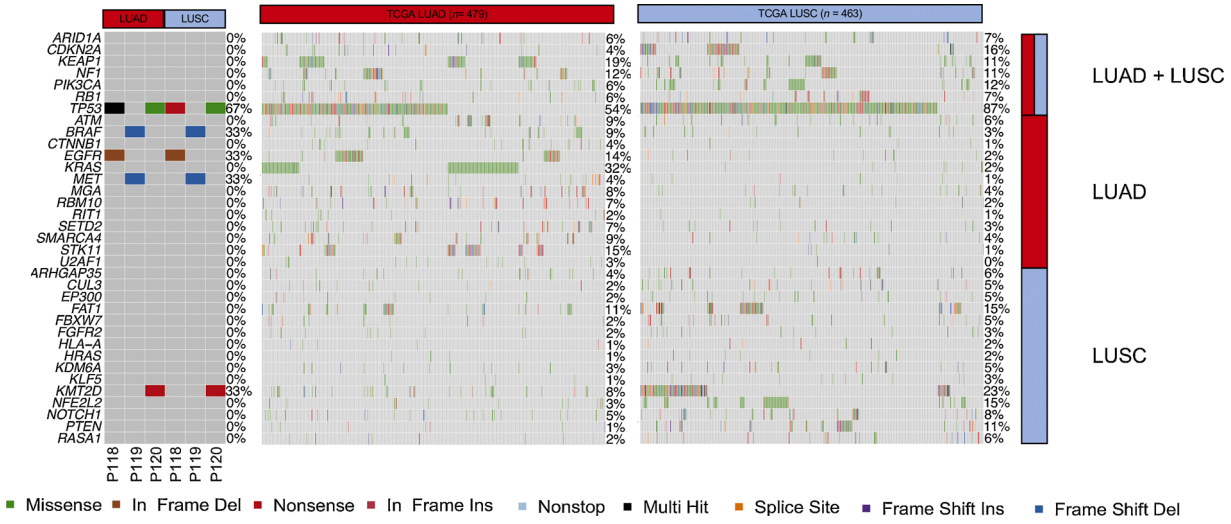

Fig. 4. Non-synonymous mutation plot and comparison with TCGA LUAD and LUSC datasets. The heatmap depicts a comparison between the non-synonymous genes in the dataset of Bailey et al. that represents the most significantly mutated genes in classic LUAD (middle) and LUSC (right) [13]. The figure shows a comparison between the three ASC patients (left), TCGA LUAD (TCGA, Nature 2014) and LUSC (TCGA, Provisional) datasets from the cBioPortal (http://cbioportal.org) Left plot LUAD = adeno component of ASC; LUSC = squamous cell carcinoma component of ASC. Order of the patients within the components of LUAD is P118, P119, P120 and in LUSC P118, P119, P120.

mutations.

Truncal copy number variations (CNVs) might also play a role as drivers of malignancy. Loss of regions at chr 3p, 15q, 19p and an amplified locus at chr 5p were identified across all samples. Losses in regions of chr 6, 17 and 20 in LUAD of P118 were normal in LUSC. LUAD P119 had private losses in regions of chr 19, whereas the LUSC component harbored private losses in chr 12. Further private losses in chr 12 were identified in P120 LUSC. Regions of chr 9 were gained in LUSC P120 but lost in the LUAD component. Notably, there was truncal loss of *STK11* at 19p13 in P118 and P120. In P120, we detected a truncal amplified region on 3q including *TP63* and *SOX2* (Fig. 3). SOX2 amplification was confirmed using FISH (Supplementary Fig. 1).

Given that truncal genomic alterations are likely acquired prior to the branching of the two components, we sought to investigate whether mutational signatures are shared or change over time (Fig. 3). For all our three ASC, we found different patterns of signatures as well as commonalities.

Trunks of all three tumors displayed signatures 1 and 4. The truncal mutations of P118 and P119 were also characterized by the APOBEC signature 13. In addition, trunks of P118 and P120 carried signature 5. The signatures changed drastically in the branches. Whereas, P119 LUAD was found to exhibit signatures 1, 2, 4 and 13 the LUSC component only exhibited signature 1 and 6. Signature 1 contributed to more than 50 % of the mutations of all LUAD/LUSC branches, except of P118 LUAD where it was not present at all. The smoking signature was also seen in both components of P120 and in P119 LUAD, but not P119 LUSC. Several signatures were observed exclusively in a single branch, including signature 13 in P119 LUAD, signature 6 in P119 LUSC and

signature 17 in P120 LUAD. Notably, signature 6 was observed in P119 LUSC, which is not common in classic LUSC, but prominent in LUAD.

4. Discussion

ASC had originally been assumed to be a mixed tumor with a polyclonal origin consisting of two separate tumors until recent gene panel sequencing demonstrated shared mutations in LUAD and LUSC [5,6]. Here we provided unequivocal evidence for a monoclonal origin of the LUAD and LUSC components in ASC based on comprehensive mutational patterns and CNVs obtained by WES.

In our study, truncal genetic alterations included not only mutations in common cancer genes such as *TP53* but also the typical driver gene mutations of LUAD in *EGFR*, *BRAF* and deletions of *STK11* (Fig. 3). This is in line with previous studies using NGS panels or selected single gene testing of the two ASC components [5,6]. In particular, activating *EGFR* mutations have been shown to be at least as common in ASC as in classical LUAD ranging from approximately 15 % in Western patients to 50 % in Asian patients, while they have been reported in only ~2% of LUSC [22–24]. This has also been emphasized by a recent study of Lin et al., who showed that the genomic ASC profiles by targeted sequencing looked more similar to classic LUAD than LUSC [6]. In accordance, typical LUAD mutations were predominant in our study. We identified only one *KMT2D* mutation as a putative LUSC driver [25,26]. *KMT2D* mutations are not exclusive for LUSC as they occur, albeit less frequently, also in LUAD according to TCGA (21 % vs. 8%) (http://cbioportal.org) [27]. In summary, the clonal relationship between the two components in ASC together with the presence of more LUAD than LUSC mutations suggest that ASC originates from an early LUAD ancestor. Interestingly, 23 lymph node metastases from 12 patients in the recent study by Lin et al. contained either LUAD or ASC (11, each), while only one consisted of pure LUSC [6]. This further supports that an early LUAD-like ancestor might not only be the driving force during tumor development but also during progression.

Tumor evolution is influenced by exogenous and endogenous mutational processes that shape the spectra of different mutational signatures [28]. It was previously demonstrated that LUAD and LUSC share common signatures of type 1 (CpG deamination and aging), 2 (APOBEC), 4 (smoking), 5 (transcriptional strand bias for T > C) 13 (APOBEC). In addition, LUAD was found to display signatures 6 (defective DNA-repair) and 17 (unknown origin) [21]. In our study, the trunks of all three ASC were dominated by aging and smoking-related signatures 1 and 4, respectively, which is partly explained by a smoking history of the patients. Interestingly, the distribution of signatures changed markedly in the LUAD and LUSC branches. This is in line with previous studies on LUAD, LUSC and breast cancer showing that mutational signatures may change from the trunk to branches [19,29,30]. Change in mutation signatures can provide additional insights into the development and evolutionary traits of malignant tumors [31,32]. Recently, Richard and colleagues found an association between mutational signatures and clinical efficacy of nivolumab, an immune checkpoint inhibitor, in lung cancer patients [33]. In our study, the trunks of all three ASC were dominated by aging and smoking-related signatures 1 and 4, respectively, which is partly explained by a smoking history of the patients. However, the distribution of signatures changed markedly in the LUAD and LUSC branches. Notably, we did not observe a systematic accumulation of the APOBEC signature, which was previously shown to drive mutagenesis and subclonal expansion in LUAD and LUSC [31]. Taken together, we found that most of the genomic alterations accumulated in the trunk before branching and changed over time. Aging and smoking-induced signatures 1 and 4 were the most prominent and present in almost all lineages suggesting a promoting role in tumor development and progression. Further studies are needed to better understand the biological significance and potential clinical impact of mutational signatures in lung cancer, and their association with histological transdifferentiation.

Our gene copy number data suggest persistent genomic instability as chromosomal aberrations are detected even after branching of the two components. The high overall concordance between the chromosomal copy number aberrations profiles of the components support our previous data from metastatic LUAD showing that most aberrant genomic events are truncal with only limited heterogeneity between primary tumors and matched metastases [34]. Nevertheless, the two ASC components had private CNVs, which were similar to the CNVs known to be typical for their pure morphological counterparts, i.e. classical LUAD and LUSC, respectively [35]. For example, the trunk of P120 and P119 LUSC had an amplified region on 3q including *SOX2*. *SOX2* expression is known as a common feature of squamous differentiation, and *SOX2* amplification occurs in 40 % of LUSC but is almost never seen in LUAD [36]. Thus, it is possible that *SOX2* amplification served as a genomic precondition to facilitate the AST of truncal LUAD to LUSC in P119 and P120. This hypothesis would be in line with previous evidence from a mouse model, in which overexpression of *SOX2* induced squamous differentiation [37,38]. In fact, AST was linked to silenced TTF-1 expression in the pre-clinical mouse model, suggesting that the differential regulation of TTF-1 and *SOX2* expression might be involved in the transformation process. In P120, AST is difficult to prove. The truncal nature of *SOX2* amplification and *KMT2D* mutation could point towards a reverse sequence with a LUSC-type ancestor clone despite the truncal *STK11* loss. Deletion of *STK11,* which we found in P118 and P120, might pinpoint another mechanism of plasticity and AST. *STK11* alterations in general, occur in up to 14 % in classic LUAD but in only 2% of classical LUSC (http://cbioportal.org) [39]. There is pre-clinical evidence from mouse models suggesting that different mechanisms in *STK11* deficiency can lead to a transition from LUAD to LUSC [40,41]. Concluding, AST is a complex process that might be caused due to several different mechanisms that require further studies.

The main limitation of this study is the low number of patients reflecting the rarity of the tumor. In fact, this is the first study to perform comprehensive WES on the two components of ASC separately. Moreover, the usage of archived FFPE blocks and contamination with non-tumor tissue negatively affect the resolution of our analysis. Nevertheless, our CNV data of *SOX2* and *STK11* support pre-clinical evidence of genomic driven mechanisms that could facilitate or mediate AST to LUSC. Although we discovered only *KMT2D* as a candidate mutation known to be typical but not exclusive for squamous differentiation, we cannot rule out a role of other mutations or mutational patterns. It is likely that AST in ASC is driven by both genetic and non-genetic mechanisms including transcriptional regulation and metabolic factors as discussed above. The role of epigenetic reprogramming has not yet been studied in the context of AST in ASC despite the paramount importance of epigenetics in shaping morphology [42].

5. Conclusion

Our whole-exome analysis showed compelling evidence for a clonal relationship between the LUAD and LUSC components of ASCs, and the emergence from a common LUAD-like ancestor clone. Even if the results are ambiguous, identification of *SOX2* amplification and *STK11* loss in two of the three LUSC components, each, supports previous pre-clinical evidence for a role of these genes in AST. Further and more comprehensive studies with a larger sample size are needed to gain a better understanding of the mechanisms that drive transformation from LUAD to LUSC or LUSC to LUAD, including transcriptomics and epigenomics.

Financial support

This work was supported by: Swiss National Science Foundation [SNF320030_162781 to L.B., PZ00P3_168165 to S.P.; the Swiss Cancer League [KFS-3995-08-2016 to S.P., KFS-4543-08-2018 to C.K.Y.N.].

CRediT authorship contribution statement

Arthur Krause: Conceptualization, Methodology, Validation, Investigation, Formal analysis, Data curation, Writing - original draft, Project administration. **Luca Roma:** Formal analysis, Data curation, Visualization. **Thomas Lorber:** Methodology, Writing - original draft. **James Habicht:** Resources. **Didier Lardinois:** Resources. **Maria Rosaria De Filippo:** Formal analysis. **Spasenija Savic Prince:** Resources. **Salvatore Piscuoglio:** Conceptualization, Writing - original draft, Supervision. **CharlotteKY Ng:** Conceptualization, Formal analysis, Writing - original draft, Supervision. **Lukas Bubendorf:** Conceptualization, Resources, Writing - original draft, Supervision, Funding acquisition.

Declaration of Competing Interest

The authors report no declarations of interest.

Acknowledgements

We acknowledge CeGaT (Tübingen, Germany) for the technical expertise in sequencing.

Appendix A. Supplementary data

Supplementary material related to this article can be found, in the online version, at doi:https://doi.org/10.1016/j.lungcan.2020.10.013.

References

[1] International Agency for Research on Cancer, Who Classification of Tumours of the Lung, Pleura, Thymus and Heart, World Health Organization, 2015.
[2] P.L. Filosso, E. Ruffini, S. Asioli, R. Giobbe, L. Macri, M.C. Bruna, A. Sandri, A. Oliaro, Adenosquamous lung carcinomas: a histologic subtype with poor prognosis, Lung Cancer 74 (2011) 25–29, https://doi.org/10.1016/j.lungcan.2011.01.030.
[3] X. Shi, S. Wu, J. Sun, Y. Liu, X. Zeng, Z. Liang, et al., PD-L1 expression in lung adenosquamous carcinomas compared with the more common variants of non-small cell lung cancer, Sci. Rep. 7 (2017), 46209, https://doi.org/10.1038/srep46209.
[4] C. Li, H. Lu, Adenosquamous carcinoma of the lung, Onco. Ther. 11 (2018) 4829–4835, https://doi.org/10.2147/ott.s164574.
[5] E. Vassella, S. Langsch, M.S. Dettmer, et al., Molecular profiling of lung adenosquamous carcinoma: hybrid or genuine type? Oncotarget 6 (2015) 23905–23916, https://doi.org/10.18632/oncotarget.4163.
[6] G. Lin, et al., Genomic origin and EGFR-TKI treatments of pulmonary adenosquamous carcinoma, Ann. Oncol. 31 (2020) 517–524.
[7] C.F.B. Kim, E.L. Jackson, A.E. Woolfenden, D. Crowley, Identification of bronchioalveolar stem cells in normal lung and lung Cancer, Cell 121 (2005) 823–835, https://doi.org/10.1016/j.cell.2005.03.032.
[8] T. Blumer, I. Fofana, M.S. Matter, et al., Hepatocellular carcinoma xenografts established from needle biopsies preserve the characteristics of the originating tumors, Hepatol Commun. 3 (2019) 971–986.
[9] S. Piscuoglio, C.K.Y. Ng, M.P. Murray, et al., The genomic landscape of male breast cancers, Clin. Cancer Res. 22 (2016) 4045–4056, https://dx.doi.org/10.1158%2F1078-0432.CCR-15-2840.
[10] C.T. Saunders, W.S.W. Wong, S. Swamy, et al., Strelka: accurate somatic small-variant calling from sequenced tumor-normal sample pairs, Bioinformatics 28 (2012) 1811–1817, https://doi.org/10.1093/bioinformatics/bts271.
[11] K. Cibulskis, M.K. Lawrence, S.L. Carter, et al., Sensitive detection of somatic point mutations in impure and heterogeneous cancer samples, Nat. Biotechnol. 31 (2013) 213–219, https://doi.org/10.1038/nbt.2514.
[12] P. Cingolani, A. Platts, L.L. Wang, et al., A program for annotating and predicting the effects of single nucleotide polymorphisms, SnpEff: SNPs in the genome of Drosophila melanogaster strain w1118; iso-2; iso-3, Fly 6 (2012) 80–92, https://doi.org/10.4161/fly.19695.
[13] M.H. Bailey, C. Tokheim, E. Porta-Pardo, et al., Comprehensive characterization of Cancer driver genes and mutations, Cell 173 (2018) 371–385, https://doi.org/10.1016/j.cell.2018.02.060, e18.
[14] R. Shen, V.E. Seshan, FACETS: allele-specific copy number and clonal heterogeneity analysis tool for high-throughput DNA sequencing, Nucleic Acids Res. 44 (2016) e131, https://doi.org/10.1093/nar/gkw520.
[15] S.L. Carter, K. Cibulskis, E. Helman, et al., Absolute quantification of somatic DNA alterations in human cancer, Nat. Biotechnol. 30 (2012) 413–421, https://dx.doi.org/10.1038%2Fnbt.2203.
[16] D.A. Landau, S.L. Carter, P. Stojanov, et al., Evolution and impact of subclonal mutations in chronic lymphocytic leukemia, Cell 152 (2013) 714–726, https://doi.org/10.1016/j.cell.2013.01.019.
[17] E. Guerini-Rocco, S. Piscuoglio, C.K.Y. Ng, et al., Microglandular adenosis associated with triple-negative breast cancer is a neoplastic lesion of triple-negative phenotype harbouring TP53 somatic mutations, J. Pathol. 238 (2016) 677–688, https://dx.doi.org/10.1002%2Fpath.4691.
[18] N. Murugaesu, G.A. Wilson, N.J. Birkbak, et al., Tracking the genomic evolution of esophageal adenocarcinoma through neoadjuvant chemotherapy, Cancer Discov. 5 (2015) 821–831, https://doi.org/10.1158/2159-8290.cd-15-0412.
[19] C.K.Y. Ng, F.C. Bidard, S. Piscuoglio, et al., Genetic heterogeneity in therapy-naïve synchronous primary breast cancers and their metastases, Clin. Cancer Res. 23 (2017) 4402–4415, https://doi.org/10.1158/1078-0432.ccr-16-3115.
[20] R. Rosenthal, N. McGranahan, J. Herrero, B.S. Taylor, C. Swanton, DeconstructSigs: delineating mutational processes in single tumors distinguishes DNA repair deficiencies and patterns of carcinoma evolution, Genome Biol. 17 (2016) 31, https://doi.org/10.1186/s13059-016-0893-4.
[21] L.B. Alexandrov, S. Nik-Zainal, D.C. Wedge, et al., Signatures of mutational processes in human cancer, Nature 500 (2013) 415–421, https://doi.org/10.1038/nature12477.
[22] X. Shi, H. Wu, J. Lu, et al., Screening for major driver oncogene alterations in adenosquamous lung carcinoma using PCR coupled with next-generation and Sanger sequencing methods, Sci. Rep. 6 (2016), 22297, https://doi.org/10.1038/srep22297.
[23] K.-H. Hsu, C.-C. Ho, et al., Identification of five driver gene mutations in patients with treatment-naïve lung adenocarcinoma in Taiwan, PLoS One 10 (2015), e0120852, https://doi.org/10.1371/journal.pone.0120852. T.-C.
[24] T.C.G.A.R. Network, The cancer genome atlas research network, comprehensive molecular profiling of lung adenocarcinoma, Nature 511 (2014) 543–550, https://doi.org/10.1038/nature13385.
[25] T.C.G.A.R. Network, The cancer genome atlas research network, comprehensive genomic characterization of squamous cell lung cancers, Nature 489 (2012) 519–525, https://doi.org/10.1038/nature11404.
[26] H. Zhang, C.F. Brainson, et al., Lkb1 inactivation drives lung cancer lineage switching governed by polycomb repressive complex 2, Nat. Commun. 8 (2017) 14922.
[27] R.L. Grossman, A.P. Heath, V. Ferretti, et al., Toward a shared vision for Cancer Genomic data, N. Engl. J. Med. 375 (2016) 1109–1112, https://doi.org/10.1056/NEJMp1607591.
[28] M. Jamal-Hanjani, G.A. Wilson, N. McGranahan, et al., Tracking the evolution of non-small-cell lung cancer, N. Engl. J. Med. 376 (2017) 2109–2121, https://doi.org/10.1056/nejmoa1616288.
[29] J.Y. Lee, M. Schizas, F.C. Geyer, et al., Lobular carcinomas in situ display intralesion genetic heterogeneity and clonal evolution in the progression to invasive lobular carcinoma, Clin. Cancer Res. 25 (2019) 674–686, https://doi.org/10.1158/1078-0432.CCR-18-1103.
[30] E.C. de Bruin, N. McGranahan, R. Mitter, et al., Spatial and temporal diversity in genomic instability processes defines lung cancer evolution, Science 346 (2014) 251–256, https://doi.org/10.1126/science.1253462.
[31] C. Swanton, N. McGranahan, G.J. Starrett, R.S. Harris, APOBEC enzymes: mutagenic fuel for Cancer evolution and heterogeneity, Cancer Discov. 5 (2015) 704–712, https://dx.doi.org/10.1158%2F2159-8290.CD-15-0344.
[32] I.B. Rogozin, Y.I. Pavlov, A. Goncearenco, et al., Mutational signatures and mutable motifs in cancer genomes, Brief. Bioinform 19 (2018) 1085–1101, https://dx.doi.org/10.1093%2Fbib%2Fbbx049.
[33] C. Richard, J.-D. Fumet, S. Chevrier, et al., Exome analysis reveals genomic markers associated with better efficacy of nivolumab in lung Cancer patients, Clin. Cancer Res. 25 (2019) 957–966, https://doi.org/10.1158/1078-0432.ccr-18-1940.
[34] T. Lorber, N. Andor, T. Dietsche, et al., Exploring the spatiotemporal genetic heterogeneity in metastatic lung adenocarcinoma using a nuclei flow-sorting approach, J. Pathol. 247 (2019) 199–213, https://doi.org/10.1002/path.5183.
[35] Z.-W. Qiu, J.-H. Bi, A.F. Gazdar, K. Song, Genome-wide copy number variation pattern analysis and a classification signature for non-small cell lung cancer, Genes Chromosomes Cancer 56 (2017) 559–569, https://doi.org/10.1002/gcc.22460.
[36] T. Tatsumori, K. Tsuta, K. Masai, et al., p40 is the best marker for diagnosing pulmonary squamous cell carcinoma: comparison with p63, cytokeratin 5/6, desmocollin-3, and sox2, Appl. Immunohistochem. Mol. Morphol. 22 (2014) 377–382, https://doi.org/10.1097/pai.0b013e3182980544.
[37] P.R. Tata, R.D. Chow, S.V. Saladi, et al., Developmental history provides a roadmap for the emergence of tumor plasticity, Dev. Cell 44 (2018) 679–693, https://doi.org/10.1016/j.devcel.2018.02.024, e5.
[38] G. Mollaoglu, A. Jones, S.J. Wait, et al., The lineage-defining transcription factors SOX2 and NKX2-1 determine lung Cancer cell fate and shape the tumor immune microenvironment, Immunity 49 (2018) 764–779, e9.
[39] E. Cerami, J. Gao, U. Dogrusoz, et al., The cBio cancer genomics portal: an open platform for exploring multidimensional cancer genomics data, Cancer Discov. 2 (2012) 401–404, https://doi.org/10.1158/2159-8290.cd-12-0095.
[40] F. Li, X. Han, F. Li, et al., LKB1 inactivation elicits a redox imbalance to modulate non-small cell lung Cancer plasticity and therapeutic response, Cancer Cell 27 (2015) 698–711, https://doi.org/10.1016/j.ccell.2015.04.001.
[41] S. Hou, S. Zou, Z. Qin, et al., Evidence, mechanism, and clinical relevance of the transdifferentiation from lung adenocarcinoma to squamous cell carcinoma, Am. J. Pathol. 187 (2017) 954–962, https://doi.org/10.1016/j.ajpath.2017.01.009.
[42] G. Mollaoglu, A. Jones, S.J. Wait, et al., The lineage-defining transcription factors SOX2 and NKX2-1 determine lung Cancer cell fate and shape the tumor immune

microenvironment, Immunity 49 (2018) 764–779, e9. https://dx.doi.org/10.1016%2Fj.immuni.2018.09.020.